Published in final edited form as:
*Heart Rhythm*. 2008 June ; 5(6): 857–860. doi:10.1016/j.hrthm.2008.03.011.

# Noninvasive Electrocardiographic Imaging (ECGI) of Epicardial Activation Before and After Catheter Ablation of Accessory Pathway in a Patient with Ebstein's Anomaly

**Subham Ghosh, MS**[F,e], **Jennifer N Avari, MD**[a], **Edward K Rhee, MD, FACC**[F,b], **Pamela K. Woodard, MD**[F,c], and **Yoram Rudy, PhD, FAHA, FHRS**[F,e,a,c]

[F] Cardiac Bioelectricity and Arrhythmia Center (CBAC), Washington University, St Louis, MO

[e] Department of Biomedical Engineering, Washington University, St. Louis, MO

[a] Division of Pediatric Cardiology, Washington University School of Medicine/St. Louis Children's Hospital, St. Louis, MO

[b] Eller Congenital Heart Center, Heart Lung Institute, St. Joseph's Hospital and Medical Center, Phoenix, AZ

[c] Mallinckrodt Institute of Radiology, Washington University, St Louis, MO

**Keywords**

Electrocardiographic Imaging (ECGI); Wolff-Parkinson-White syndrome; Ebstein's anomaly; Ablation

Ebstein's anomaly (1) is characterized by abnormal development of the tricuspid valve with the septal (and often posterior) leaflets of the valve displaced into the right ventricle (RV). The abnormal development of the tricuspid valve is often associated with several conduction abnormalities, including delayed intra-atrial conduction, right bundle branch block (RBBB) (2,3), and ventricular pre-excitation (4). Absence of a RBBB pattern during sinus rhythm on a baseline ECG suggests the presence of an atrio-ventricular accessory pathway (AP) in patients with Ebstein's anomaly. Often, successful catheter ablation of an AP results in a complete or partial RBBB pattern on the post-ablation 12-lead ECG in 94% of cases (5). However, changes in the activation of the heart following a successful catheter ablation of AP in a patient with Ebstein's anomaly have never been studied with epicardial activation imaging techniques.

Electrocardiographic imaging (ECGI) (6,7) is a novel noninvasive imaging modality for cardiac electrophysiology. ECGI can image cardiac activity on the epicardial surface of the heart from body-surface potentials measured with 250 electrodes together with heart-torso anatomic information obtained from a thoracic ECG-gated CT. It has been validated with intra-operative mapping data in humans (8). It has also been applied in humans to image the electrophysiologic substrate and cardiac excitation under normal and various pathophysiologic conditions (6–11).

Corresponding Author:Yoram Rudy, Ph.D., Cardiac Bioelectricity Center, 290 Whitaker Hall, Campus Box 1097, One Brookings Drive, St Louis, MO 63130-4899. rudy@wustl.edu.

Disclosures: Y. R. chairs the scientific advisory board and holds equity in CardioInsight Technologies (CIT). CIT does not support any research conducted by Y.R., including that presented here.

## Case

A 16 year old female was referred to Cardiology clinic for chief complaint of palpitations. Her evaluation included an echocardiogram that revealed mild inferior displacement of the septal leaflet of the tricuspid valve consistent with mild Ebstein's anomaly and mild tricuspid regurgitation with normal ventricular systolic function. A resting 12-lead ECG demonstrated pre-excitation with her delta-wave morphology (delta wave positive in lead I and negative in lead II, Figure 1 top panel) indicating a subepicardial pathway inside the coronary venous system (12). She was referred to this institution for transvenous catheter ablation.

A day prior to her electrophysiologic study (EPS), she underwent body surface potential mapping (BSPM) with 250 electrodes arranged in strips, covering the front and back of her torso, and a thoracic CT scan gated to 70% of the ECG R-R interval. Skin markers were adhered to her torso to mark the layout of the strips for future application at the same locations. Body surface potentials were baseline corrected, filtered to remove 60 Hz and ECGI reconstructed ventricular activation map was produced during a single pre-excitation beat.

Figure 2 shows the ECGI imaged ventricular activation sequence during a pre-excitation beat (Panel A, RAO View, Panel B, Left Lateral View). The map shows activation initiating from the right posterolateral region (red, 7 o'clock around the tricuspid valve annulus, marked by asterisk). A single activation front originating from this site excites the entire ventricular epicardium, the posterolateral RV wall being the earliest to activate and the LV apex and lateral wall being the latest to activate (dark blue). There is no evidence of fusion with activation from the conduction system, a property characteristic of a right-sided AP.

The following day she underwent EPS and ablation. At baseline, there was pre-excited sinus rhythm at 68 beats per minute with a PR interval of 114 msec, QRS duration of 116 msec and QT interval of 452 msec. Intracardiac measurements included an atrial-His (AH) interval of 83 msec and a His-ventricle (HV) interval of 16 msec confirming pre-excitation. A hand injection coronary sinus venogram (Figure 3, panel C) was taken through an 8 French Mullins sheath to delineate the plane of the AV annulus. A second injection in the body of the RA showed atrialization of the RV with an extremely narrow distance between the tricuspid valve annulus and the epicardial lesser cardiac vein. Next, 3-dimensional electroanatomical mapping (Biosense, CARTO) was performed for localization of the AP. Earliest activation was found to occur at the posterolateral area of the annular plane, approximately 7o'clock around the tricuspid annulus.

In order to facilitate induction of tachycardia, an isoproterenol infusion was started at 0.01 mcg/kg/minute and atrial extrastimulus testing was started. There was induction of sustained supraventricular tachycardia (SVT) at 177 beats per minute with a narrow QRS complex. A CARTO map (Figure 3, Panel A) was constructed during SVT, which mapped the retrograde atrial signal to the right posterolateral tricuspid valve at approximately 7:45 position as seen on the LAO projection (Figure 3, panel B) indicating a right posterolateral AP. There was no evidence of a second AP or AV nodal reentry. Cryoablation system was used due to the close proximity of the ablation target to the right coronary artery. Prior to cryoablation, a well fused VA signal was seen with a local VA time of 84 msec during free running SVT. A full power cryolesion was applied at the target site which resulted in termination of SVT within 8 seconds. No pre-excitation was observed after this ablation. Four more insurance lesions were applied in the vicinity of the first acutely successful lesion, again with no inducible tachycardia and no pre-excitation. Following successful ablation, routine testing was done to rule out the presence of a second pathway. Atrial extrastimulus testing was repeated in the presence and absence of isoproterenol. There was no pre-excitation with atrial pacing and no evidence of dual AV node physiology or other SVT mechanisms. Ventricular pacing in the absence of isoproterenol

showed VA Wenckebach at a paced cycle length of 700msec indicating successful interruption of retrograde pathway conduction. An adenosine challenge was given after 1 hour observation period with 6 mg of intravenous adenosine. This produced AV and VA block. Final rhythm at the end of the case was non preexcited sinus rhythm at 75 beats per minute with a PR interval of 147 msec, QRS duration of 90 msec, and QT interval of 416 msec. The AH interval was 92 msec and the HV interval was now normal at 40 msec indicating no pre-excitation.

One hour after successful interruption of her AP, electrode strips were applied to her torso, guided by the skin markers and the digital photographs taken during her 'pre-ablation' ECGI. Care was taken to ensure that orientation and layout of the strips remain the same as that during the pre-ablation mapping. Body-surface potentials were recorded with the patient in the same supine position as in the ECGI study prior to ablation. This method enabled us to use the patient specific geometry (heart-torso geometry acquired prior to ablation) and avoided the need for repeating the CT scan during the post-ablation follow-up with ECGI.

Her post-ablation ECGI activation maps are shown in Figure 2, panels C (RAO view) and D (left lateral view), respectively. Activation of the right posterolateral region (earliest to activate pre-ablation) is now reversed and occurs later (blue, panel C). Earliest activation post-ablation is in an anterior paraseptal region and an inferior antero-apical region of the LV (red areas, panel C). Figure 2, panels E (RAO view) and F (left lateral view), show the ECGI imaged epicardial potential map post ablation, 38 ms after onset of QRS. A local potential minimum (blue, black asterisk) develops on the anterior RV surface, midway between the anterior RV base and the LAD, indicating RV breakthrough (RVBT). This earliest RVBT occurs 38 msec after QRS onset on the body-surface ECG and 13 msec after the earliest LV epicardial breakthrough. Conduction in the RV is slow as evident from crowding of isochrones, with the right ventricular outflow tract (RVOT) region being the latest to activate (deep blue, panel C). Activation of the LV (left lateral view, panel D) occurs in a normal apex-to-base fashion, with the basal posterolateral area of the LV being the last to activate (deep blue).

## Discussion

Both ECGI (6,7) and invasive epicardial mapping (13) have shown that during normal excitation, earliest epicardial activation occurs on anterior RV, 18–20 msec from onset of QRS. The location and timing of this RV breakthrough (RVBT) is indicative of normal conduction system function and excitation via the right bundle branch (RBB). After the first RVBT, additional breakthroughs appear at epicardial RV sites which results in synchronized activation of anterior RV as well as anterior septal aspects of the epicardium (regions adjacent to the LAD) (6,7) . The first LV breakthrough typically lags the RVBT by about 10 ms in normals (7). However, in the present case, in the post-ablation rhythm, only one area of early RV epicardial activation is seen (yellow, panel C, Figure 2), occurring 13 ms after the earliest LV activation and 38 ms after onset of QRS. The RAO view of the potential map (panel E, Figure 2) shows the site of potential minimum (RVBT) marked by a black asterisk. The RVBT site is also marked with a black asterisk on the RAO view of the post-ablation activation map in panel C, Figure 2. This breakthrough site is located on the anterior epicardium midway between the RV base and the LAD, a typical location of RVBT indicative of conduction through the RBB (6,7,13). However, its delayed appearance (38 ms after QRS onset and 13 ms after the earliest LV activation) suggests that RBB conduction in this case is slower compared to normal where the earliest RVBT occurs 18–20 ms after QRS onset. Moreover, parts of apical RV and paraseptal aspects of the epicardium are late to activate (blue areas in the RAO view, panel C), which indicates possible abnormalities of conduction in the RV and septum, compared to normal activation (6,7).

The post-ablation 12-lead ECG, though not showing typical features of a complete RBBB with a wide QRS (> 120 ms), shows notched R waves in leads V1 and V2 (insets, bottom panel, Figure 1) with a QRS duration of 90 ms and non-specific ST abnormality. A notched R-wave in precordial leads V1 or V2 with or without associated s or S waves in standard leads I, II, III and aVF may indicate RV conduction delay (14). Also, the QRS duration for partial RBBB has been reported to be 90–120 ms (14). While some of these features on the 12-lead ECG may overlap with normal variants or non-specific abnormalities, ECGI can complement the routine ECG in such cases by providing a more detailed and quantitative information about regional ventricular activation.

We conclude from the EP testing and post-ablation ECG that the patient had a successful ablation of her single AP and there was no residual pathway conduction or a second AP. The QRS complexes on surface 12-lead ECG post-ablation were identical to those encountered upon initiation of SVT in the cardiac catheterization laboratory. We can conclude from this that there is neither an injured pathway nor a second AP. If there was either an injured or a second AP, there would be a discrepancy between the QRS morphologies in SVT and in the post-ablation sinus rhythm. Also, the adenosine challenge demonstrated bidirectional AV and VA block, consistent with only AV nodal conduction.

The ECG algorithm (positive delta wave in lead I, negative delta wave in lead II) (12) localized the pathway to a subepicardial location. Noninvasive ECGI activation maps localized the AP to a right posterolateral position around the tricuspid valve annulus. The ECGI prediction agreed with invasive electroanatomic mapping and a successful ablation site which was recorded at the right posterolateral region, 7 o' clock around the tricuspid valve annulus. While ECGI in conjunction with invasive electroanatomic mapping guided the ablation procedure, the follow-up images showed for the first time how the activation sequence changes following ablation of an AP in a heart with Ebstein's anomaly. Prior to ablation, during the pre-excitation rhythm, activation spread from the pre-excited region and was uniform throughout the ventricular epicardium (both RV and LV) without any apparent fusion with activation via the normal conduction system. Epicardial right ventricular breakthrough (RVBT) is indicative of conduction via the AV node and the Purkinje system. Studies by Liebman *et al*(15) have shown evidence of lack of epicardial RVBT for WPW right-sided and anteroseptal pathways. This may be explained by the proximity of the AP to the right bundle branch. However, epicardial activation map may not show fusion if the pre-excitation activation wave-front arrives at the epicardial surface at the same time as excitation via the conduction system at the areas of epicardial breakthrough. This may be a possible cause for apparent lack of fusion in the pre-ablation activation image. After successful catheter ablation of the AP, earliest activation occurred at two LV sites along with a slightly delayed RVBT. While conduction in LV was normal, RV was characterized by slow conduction.

The Arruda algorithm (12) initially reported an overall sensitivity of 90% and specificity of 99% in predicting location of APs and 100% specificity and sensitivity for subepicardial pathways in hearts with a single AP. This and other ECG-based algorithms have been reported to be inaccurate in children and patients with congenital heart disease (16). This case illustrates that in a heart with a structural abnormality (Ebstein's anomaly) and AP, the predicted location of AP from this algorithm may not be correct. ECGI, which incorporates patient-tailored torso-heart anatomy information, proved to be more accurate than the 12-lead ECG in this case, as validated by catheter mapping and successful cryoablation. This report suggests that such cases may benefit from imaging with ECGI prior to EPS and ablation.

## Acknowledgments

The study was supported by Merit Award R37-HL-033343 and Grant R01-HL-49054 from the National Heart, Lung, and Blood Institute to Y. Rudy. Dr. Rudy is the Fred Saigh Distinguished Professor at Washington University in St. Louis.

## References

1. Brickner EM, Hillis DL, Lange RA. Congenital Heart Disease in Adults-Second of Two parts. N Engl J Med 2000;342:334–342. [PubMed: 10655533]
2. Van Lingen B, Baverfeld S. The electrocardiogram in Ebstein's anomaly of tricuspid valve. Am Heart J 1995;50:13–23. [PubMed: 14387934]
3. Macruz R, Perloff JK, Case RB. A method for the Electrocardiographic recognition of atrial enlargement. Circulation 1958;17:887–889.
4. Smith WM, Gallagher JJ, Kerr CR, et al. The electrophysiologic basis and management of symptomatic recurrent tachycardia in patients with Ebstein's anomaly of the tricuspid valve. Am J Cardiol 1982;49:1223–1234. [PubMed: 7064845]
5. Iturralde P, Nava S, Gabriel S, et al. Electrocardiographic Characteristics of Patients with Ebstein's Anomaly Before and After Ablation of an Accessory Atrioventricular Pathway. J Cardiovasc Electrophysiol 2006;17:1332–1336. [PubMed: 17239096]
6. Ramanathan C, Ghanem RN, Jia P, et al. Noninvasive Electrocardiographic imaging for cardiac electrophysiology and arrhythmia. Nat Med 2004;10:422–428. [PubMed: 15034569]
7. Ramanathan C, Jia P, Ghanem RN, et al. Activation and repolarization of the normal human heart under complete physiological conditions. Proc Nat Acad Sci U S A 2006;103:6309–6314.
8. Ghanem RN, Jia P, Ramanathan C, et al. Noninvasive electrocardiographic imaging (ECGI): comparison to intraoperative mapping in patients. Heart Rhythm 2005;2:339–354. [PubMed: 15851333]
9. Jia P, Ramanathan C, Ghanem RN, et al. Electrocardiographic imaging of cardiac resynchronization therapy in heart failure: observation of variable electrophysiologic responses. Heart Rhythm 2006;3:296–310. [PubMed: 16500302]
10. Intini A, Goldstein RN, Jia P, et al. Electrocardiographic imaging (ECGI), a novel diagnostic modality used for mapping of focal left ventricular tachycardia in a young athlete. Heart Rhythm 2005;2:1250–1252. [PubMed: 16253916]
11. Wang Y, Cuculich PS, Woodard PK, et al. Focal atrial tachycardia after pulmonary vein isolation: noninvasive mapping with electrocardiographic imaging (ECGI). Heart Rhythm 2007;4:1081–1084. [PubMed: 17675084]
12. Arruda MS, McClelland JH, Wang X, et al. Development and validation of an ECG algorithm for identifying accessory pathway ablation site in Wolff-Parkinson-White syndrome. J Cardiovasc Electrophysiol 1998;9:2–12. [PubMed: 9475572]
13. Durrer D, van Dam RT, Freud GE, et al. Total excitation of the isolated human heart. Circulation 1970;41 :899–912. [PubMed: 5482907]
14. Moore EN, Boineau JP, Patterson DF, et al. Incomplete Right Bundle-Branch Block: An Electrocardiographic Enigma and Possible Misnomer. Circulation 1971;44:678–687. [PubMed: 4255293]
15. Liebman J, Zeno JA, Olshansky B, et al. Electrocardiographic Body Surface Potential Mapping in the Wolff-Parkinson-White Syndrome : Noninvasive Determination of the Ventricular Insertion Sites of Accessory Atrioventricular Connections. Circulation 1991;83:886–901. [PubMed: 1999038]
16. Bar-Cohen Y, Khairy P, Morwood J, et al. Inaccuracy of Wolff-Parkinson-White Accessory Pathway Localization Algorithms in Children and Patients with Congenital Heart Defects. J Cardiovasc Electrophysiol 2006;17:712–716. [PubMed: 16836664]

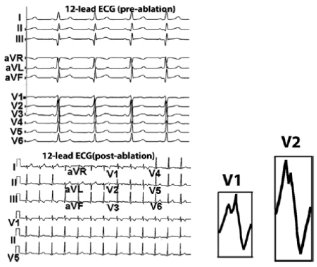


**Figure 1.**

Top Panel : Patient's 12 lead ECG before ablation. Note the positive delta wave in lead I and negative delta-wave in lead II, indicating a subepicardial posteroseptal location of the AP insertion site based on the Arruda algorithm. Bottom Panel: 12-lead ECG after successful ablation (no delta waves). Unexpectedly, a complete right bundle branch block (RBBB) pattern with a wide QRS (> 120 ms) is not noted. However, R wave in leads V1 and V2 (insets) is notched, with a post-ablation QRS duration of 90 ms and non-specific ST abnormality.

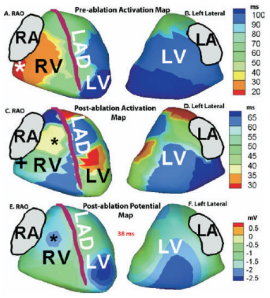


**Figure 2.**

Right Anterior Oblique (RAO) and left lateral views of ECGI imaged activation (isochrone) map before (panels A and B) and after (panels C and D) ablation. Post-ablation ECGI imaged epicardial potential maps, 38 ms after QRS onset, are shown in panels E (RAO view) and F (left lateral view). Pre-ablation, earliest activation occurs at a right posterolateral area around the tricuspid valve annulus (Panel A, red region; earliest site marked by asterisk) Post-ablation, (panel C, blue, '+') late activation occurs at the pre-ablation region of earliest activation. Earliest activation of RV (Panel C, yellow) is delayed compared to LV activation. Earliest right ventricular breakthrough (RVBT) occurs 38 ms after onset of QRS, as indicated by a negative potential minimum (blue, black asterisk, panel E) on the anterior RV epicardial surface. The site of RVBT is also marked with a black asterisk on the RAO view of the post-ablation activation map in panel C.

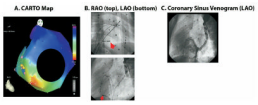


**Figure 3.**

A. Three dimensional electroanatomical map (CARTO) of retrograde atrial activation during SVT as seen in the RAO projection. The area of earliest activation (in red) occurs on the anatomic tricuspid valve annulus in the posterolateral region. B. Site of successful ablation. RAO and LAO projections show the distal tip of the ablation catheter (marked by arrow) between the 7–8 o'clock position on the tricuspid valve annulus. Other reference catheters include a coronary sinus catheter, a His catheter, and a RV catheter. C. Coronary sinus (CS) venogram in LAO projection, after injection at the mouth of the CS; it shows opacification of the mouth of CS around the posterior mitral valve and the lesser cardiac vein running around the posterior tricuspid valve.